

# A Microfabricated Wet-Spinning Apparatus To Spin Fibers of Silk Proteins. Structure–Property Correlations

Oskar Liivak, Amy Blye, Neeral Shah, and Lynn. W. Jelinski\*

Center for Advanced Technology in Biotechnology, Cornell University, Ithaca, New York 14853

Received November 4, 1997; Revised Manuscript Received February 19, 1998

**ABSTRACT:** A microfabricated spinneret is described that is capable of spinning meters of fibers from solutions containing as little as 10 mg of purified protein. Using the spinneret, regenerated *Bombyx mori* fibers were made using various processing parameters. A log–linear relationship was found between the maximum stress sustained by the regenerated fibers and their diameters. Solid state  $^{13}\text{C}$  NMR was used to determine the effects of spinneret diameter and postspinning draw ratio on the secondary structure of the alanine residues in the silk protein. The relationship between the secondary structure of the alanine residues and the maximum stress of the silks was also examined. The results suggest that a relatively high fraction of the alanine residues in the silks must be in the  $\beta$ -sheet conformation ( $>65\%$ ) in order to produce the highest stress fibers. However, the fraction of alanine residues in the  $\beta$ -sheet conformation does not uniquely determine the maximum stress of a fiber; it is suggested that orientation of these  $\beta$ -sheets is also an important parameter.

## Introduction

Silk protein fibers have excellent mechanical properties. For example, the combination of high stress and strain properties of the dragline silk of the spider *Nephila clavipes* gives these fibers one of the highest energies to break of any known polymer fiber. With advances in biotechnology, it is possible to consider the prospect of man-made and designed genetically engineered protein fibers. Recently, Kaplan<sup>1</sup> and Lewis<sup>2</sup> demonstrated that it is possible to produce tens of milligrams of genetically engineered silklike proteins whose compositions are based on consensus sequences of the spider proteins. Now the hurdle lies in being able to spin small amounts of the genetically engineered proteins into fibers whose mechanical properties can be tested. Current spinnerets require the use of relatively large amounts of material ( $>1$  g) for each run. However, obtaining gram-scale quantities of genetically engineered proteins is prohibitively expensive and time-consuming, especially during the early research phases of protein polymer development.

To overcome this obstacle, microfabricated spinnerets were constructed using silicon microfabrication methods. These spinnerets allow for the production of meters of fiber from solutions containing as little as 10 mg of protein. This development enables researchers to rapidly and efficiently assess the vast array of possible genetically engineered protein sequences without the burden of producing gram quantities per trial.

The spinneret described here was validated and tested by producing regenerated fibers from the dissolved silk protein from the silk worm *Bombyx mori*. (*B. mori* protein is readily available in large quantities and was used here as a model for *N. clavipes*.) The regenerated silk fibers and the native silk worm fibers were then studied by solid-state  $^{13}\text{C}$  NMR and mechanical testing.  $^{13}\text{C}$  chemical shifts are sensitive to the secondary structure of the protein residues.<sup>3,4</sup> It has been shown that *B. mori* fibers can be found in two dimorphic

structures silk I and silk II.<sup>4</sup> The silk II form is identified by the  $^{13}\text{C}$  chemical shifts of Gly, Ser, and Ala that are indicative of  $\beta$ -sheets, while the silk I form produces chemical shifts that are associated with a loose helix. Of these conformationally sensitive  $^{13}\text{C}$  signals, the  $\text{C}_\beta$  of the alanine residues gives both an intense peak and it furthermore has the largest chemical shift difference between conformations. Correlations were also made between the fiber diameter, draw ratio,  $\beta$ -sheet content of the alanine residues and maximum stress.

## Experimental Section

**Nanofabrication of Spinneret.** Spinnerets with controlled apertures were made at the Cornell Nanofabrication Facility according to the scheme outlined in Figure 1. A polished 3-in. wafer was coated on both sides with a 1500 Å thickness of silicon nitride using plasma-enhanced chemical vapor deposition. Both the edges and the bottom of the wafers were coated with front side coating (FSC, Shipley). The FSC-coated wafer was heated to 90 °C for 30 min in air. The wafer was primed for photoresist with hexamethyldisilazane (HMDS). A 20% HMDS solution in propylene glycol monomethyl ether acetate (PGMEA, Shipley) was applied to the wafer for 10 s. The wafer was then spun to 4000 rpm for 30 s and a layer of Shipley 1813 photoresist was spun onto the wafer at 4000 rpm for 30 s. The photoresist-coated wafer was heated to 90 °C for 30 min. The photoresist was exposed at 405 nm for 1.5 s using a HTG contact aligner with a Cr 5-in. square mask. The patterned photoresist was developed in tetramethylammonium hydroxide (Shipley MF 312) diluted 1:1 in deionized water (DI) for 1 min. The photoresist pattern was examined for aberrant flecks that were hand-repaired by recoating with photoresist. The sides of the wafer were again coated with FSC and baked for 30 min at 90 °C.

The silicon nitride window was removed with a 5 min treatment by a Plasma Therm 72 reactive ion etcher. The remaining photoresist was removed using a 1-min acetone bath. The wafer was anisotropically etched with a 85 °C, 30% KOH solution for 3.5 h. The remaining protective silicon nitride layers were removed using a Plasma Therm 72 reactive ion etcher for 5 min on both sides of the wafer. Finally, the wafer was scribed and broken into individual chips for use in the spinneret assembly.

\* To whom correspondence should be addressed.

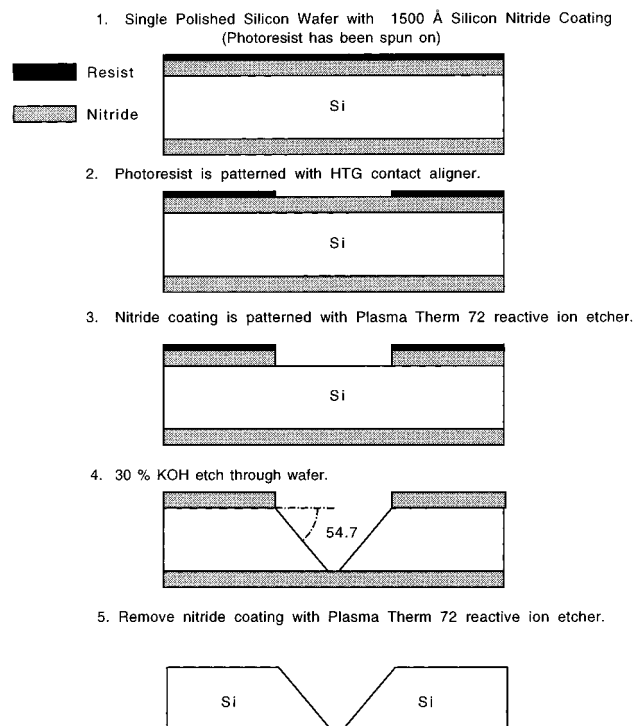


**Figure 1.** Overall scheme for producing the small apertures that are the critical components of the spinnerets. The key process is step 4, the anisotropic etch of silicon by concentrated KOH.

Using this method, a single three-inch silicon wafer was patterned to produce five sets of five apertures with 80-, 100-, 120-, 140-, and 160- $\mu\text{m}$  square openings. The apertures were characterized by light microscopy. The typical standard deviation in the final aperture dimensions was 7  $\mu\text{m}$ . The largest contribution to this error was due to variations in the thickness across the wafer.

**Preparation of *B. mori*/HFIP Solution.** Solutions of *B. mori* silk solution in hexafluoro-2-propanol (HFIP) were prepared according to the method of Lock.<sup>5</sup> Five grams of raw *B. mori* silk yarn (gift of the American Silk Association) were degummed by refluxing for 1.5 h in 100 mL of DI containing 0.32 g of sodium laurel sulfate (Aldrich) and 0.06 g of sodium carbonate (Fisher). The silk was then rinsed twice in 400 mL of DI at 70 °C, and the silk was added to 100 mL of DI with 0.03 g of sodium carbonate and refluxed for 1 h. The silk was rinsed in 400 mL of 50 °C DI. Finally, the silk was soaked in methanol for 0.5 h and left to air-dry. This produced 3.97 g of degummed silk fibroin.

The degummed silk fibroin (3.97 g) was added to 20.0 mL of DI and 24.5 g of LiBr (Aldrich). After the silk dissolved, the solution was placed in two 23-mm 8000-Da cutoff dialysis bags. The bags were dialyzed against five changes of 5 L each DI at room temperature over a 24-h period. The contents of the dialysis bags was cast onto a polyethylene sheet. After the solution dried, 3.1 g of cast silk film was recovered.

The cast film was dissolved in HFIP and filtered through a Gelman glass fiber Acrodisc syringe filter (Fisher) to remove any remaining insoluble particles. The typical working concentration for spinning fibers was 2.5% w/w silk fibroin in HFIP.

The process of dissolution with a salt and subsequent dialysis is necessary because *B. mori* fibroin treated in this way is soluble in HFIP, whereas normal untreated *B. mori* fibroin is insoluble.<sup>5</sup>

**Spinning Apparatus and Methods.** Figure 2 is a drawing of the jig designed to hold the micromachined apertures and connect them to a syringe pump. The figure shows an aperture already in place in the jig. Before the syringe containing the silk solution is attached, the jig is filled with

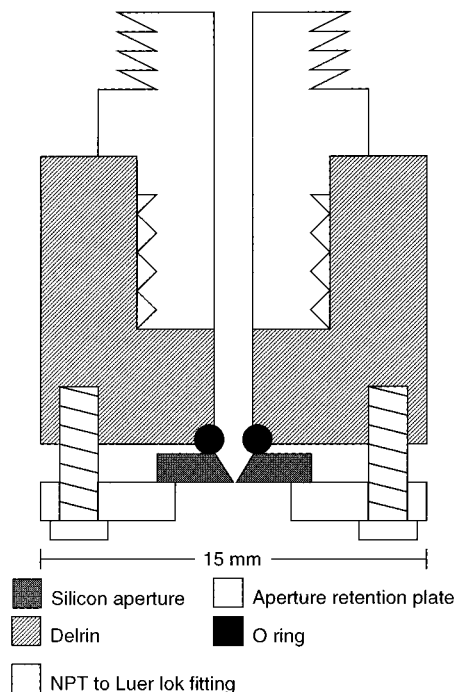


**Figure 2.** Cross-sectional view of the jig designed to hold the micromachined apertures. A syringe is attached to the Luer lock fitting on the end of the spinneret. Solution is forced out of the syringe, through the spinneret, and ultimately out through the small aperture. The 15-mm bar gives an overall scale to the spinneret, but the individual components are not drawn to scale.

HFIP. This avoids air bubbles from being pumped out of the jig. In addition, once the silk solution is loaded into the syringe, a small plug of HFIP (~0.1 mL) is drawn carefully into the syringe to prevent clogging of the jig. The syringe containing the silk solution is then attached to the jig. A syringe pump forces the solution out through the aperture and into a 30 cm column of neat methanol. The initial flow rate is generally 15  $\mu\text{L/s}$ . Although the initial flow is rather turbulent, within 2 s the system settles into a steady flow and the flow rate is lowered to 6  $\mu\text{L/s}$ . The protein is insoluble in the methanol, and it immediately coagulates into a fiber. The fibers are wound onto a home-built drawing device, drawn variable amounts within 2 h of formation, and soaked overnight in methanol. The fibers are then dried and annealed in a vacuum oven at 40 °C for 1 h.

**Spinning Statistics.** A typical run starts with 0.4 mL of 2.5% w/w silk in HFIP solution (16 mg of protein). From such a run, 8.5 mg of fiber (~50%) would be recovered. For a 140- $\mu\text{m}$  aperture and with our standard conditions, 3-m lengths of fiber of ~60  $\mu\text{m}$  diameter were produced.

**Instron Measurements.** Mechanical testing of the silk samples was performed on an Instron in a climate-controlled room (70 F, 65% RH). All samples were equilibrated in the controlled environment for at least 24 h before testing. All samples have a gauge length of 5 mm and were tested with a crosshead speed of 2 mm/min. The diameter of each sample was determined using an optical microscope with a calibrated stage micrometer. The maximum stress was calculated from the ratio of the maximum load sustained by the fiber divided by the initial cross-sectional area of the fiber. Calculation of the area assumed a circular cross-section for the fibers.

**NMR Spectroscopy.** Solid-state  $^{13}\text{C}$  spectra were obtained on a home-built spectrometer operating at 90.556 MHz for  $^{13}\text{C}$ . A Doty magic angle spinning probe was used. Randomized fiber samples were loaded into a 5-mm  $\text{ZrO}_2$  rotor with Kel-F end caps. All spectra were obtained using a cross-polarization pulse sequence and with magic-angle spinning at 5 kHz. Cross-polarization was achieved by satisfying the Hartman-Hahn condition at 53.9 kHz with a  $^{13}\text{C}$ - $^1\text{H}$  contact time of 2.5

ms. A 5.2-ms pulse was used for the initial 90° pulse. During the  $^{13}\text{C}$  acquisition the protons were decoupled at 95 kHz. The spectral width was 30 kHz, and the relaxation delay was 2 s. Chemical shifts were referenced to adamantane before and after the spectrum of each silk sample was obtained; no drift was observed. The adamantane reference peaks were taken as 29.5 and 38.56 ppm from TMS.

**Analysis of NMR Data.** Code was written to fit the  $\text{C}_\beta$  alanine region of the spectra to two Gaussians. The program used the "n2f" fitting routine from the PORT Library (AT&T Bell Laboratories, Murray Hill, NJ).<sup>6</sup> The program required operator-supplied initial estimates of the position, amplitude, and width of the two Gaussians as well as the height of the spectrum's baseline. After the fit parameters were maximized, the initial guesses were varied considerably to check that the program converged on the same set of optimal parameters.

The program consistently found that the peaks of the Gaussians were located at 20.4 and 17.6 ppm. The Gaussian centered at 20.4 ppm is the signal arising from alanine residues in  $\beta$ -sheet conformation.<sup>3,4</sup> The Gaussian at 17.4 ppm is attributed to alanine side chains in non- $\beta$ -sheet conformations. The ratio of the area of the Gaussian at 20.4 ppm to the area of the total combined Gaussians is the fraction of alanine residues in the protein that reside in  $\beta$ -sheet conformations.

## Results and Discussion

### Spinning Fibers from Ten Milligrams of Protein.

The spinneret described in Figures 1 and 2 is capable of spinning very small quantities of protein into a fiber. As such, it is ideal for research into silk fiber formation in both natural silk proteins and in genetically engineered silk proteins.

The key to this process is the anisotropic etching of Si by concentrated KOH. At 85 °C, a 30% KOH solution etches the  $\langle 100 \rangle$  and the  $\langle 110 \rangle$  faces of silicon over 300 times faster than the  $\langle 111 \rangle$  direction. Standard  $\langle 100 \rangle$  silicon wafers are cut so that the  $\langle 100 \rangle$  direction lies normal to the surface of the wafer. As shown in Figure 1, step 4, the KOH etches at an angle of 54.7° below the plane of the wafer. With the known thickness of the wafers and the known angle of etching, one can determine the final aperture size by patterning the properly sized window. If a square window is patterned into the silicon nitride, then the final small aperture will also be square.

It is thought the loss of 7.5 mg of protein (ca. 50%) in the example described in the Experimental Section, Spinning Statistics, is composed mostly of a loss due to the solution that is left in the jig when the syringe has exhausted its travel. These losses could be further minimized by reducing the dead volume left inside the jig and its various components; work along these lines is underway. In addition, such losses are systematic losses and not fractional losses; thus by spinning larger volumes, one would obtain higher yields.

**Maximum Stress and Diameter of Fibers.** Figure 3 displays maximum stress vs diameter for all fiber samples (both drawn and undrawn). Note that results for both degummed native *B. mori* and regenerated *B. mori* have been included. Figure 3 shows that there is a linear relationship between the logarithm of the maximum stress and the diameter of the fiber, and that the best regenerated fibers approach the maximum stress measured for native *B. mori*. In general, it has been established that such trends in fibers are partially the result of an increase in orientation.<sup>7</sup> The smaller diameter fibers could accomplish this by having a higher ratio of skin to core and the smaller fibers made from

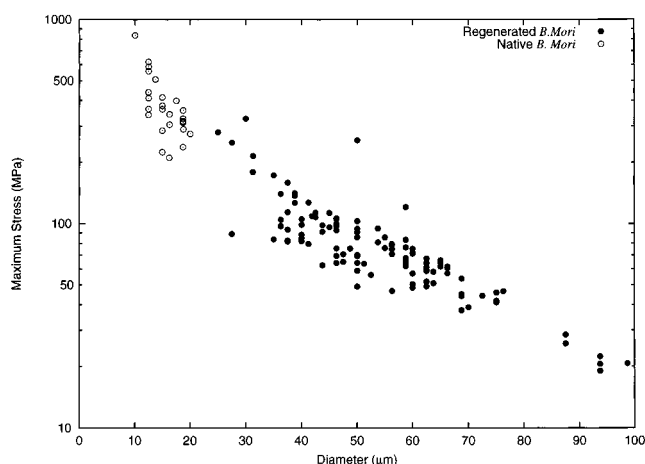


**Figure 3.** Plot of the maximum stress sustained by the fibers versus diameter. Regenerated *B. mori* data points are the filled circles; open circles correspond to native *B. mori* samples.

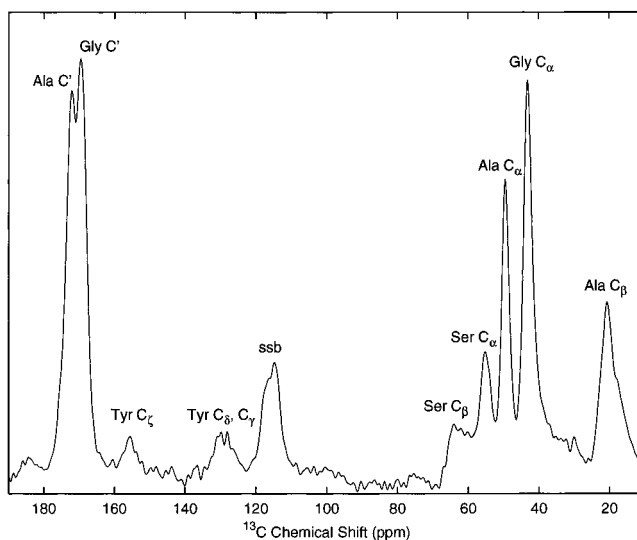


**Figure 4.** Solid-state  $^{13}\text{C}$  NMR spectrum of native *B. mori* silk fibers. Peaks marked ssb correspond to spinning sidebands of the carbonyl groups.

smaller apertures experience greater shear at the aperture.<sup>8,9</sup>

It is noteworthy that the native silk fibers from *B. mori* lie on the same line as do the regenerated fibers. The native fibers have been processed in a radically different way and yet they still follow the same trend between stress and diameter as do the regenerated fibers. This result suggests that the micromachined spinning apparatus and spinning process are able to capture some of the main features of the natural process.

**Correlation between  $\beta$ -Sheet Content and Macroscopic Processing Parameters.** Both draw ratio and aperture size were varied systematically for various runs of regenerated fiber production. Solid-state  $^{13}\text{C}$  NMR was used to investigate the effects that these macroscopic parameters have on the secondary structure of the alanine residues of the silk protein.

Figure 4 shows a typical solid-state  $^{13}\text{C}$  NMR spectrum for native *B. mori* silk. Assignments were made according to the literature.<sup>4</sup> Salient to further analysis is the fact that the methyl group of alanine (the most upfield peak) has a shoulder on it. The peak centered at 20.4 ppm is assigned to residues in a  $\beta$ -sheet

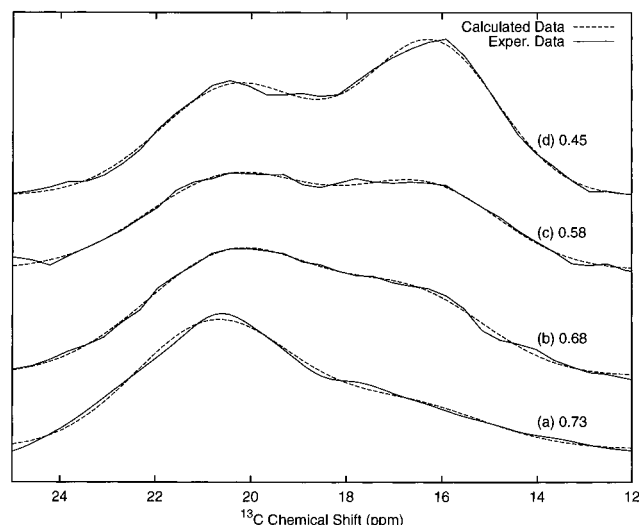


**Figure 5.** Expanded  $^{13}\text{C}$  NMR spectra of the methyl alanine-region for four silk samples: (a) native *B. mori* silk fibers; (b)–(d) regenerated *B. mori* silk fibers. Solid lines correspond to the experimental data; the best fits to each spectrum are shown as dotted lines. The numbers on each spectrum are the calculated fraction of alanine residues found in  $\beta$ -sheets.

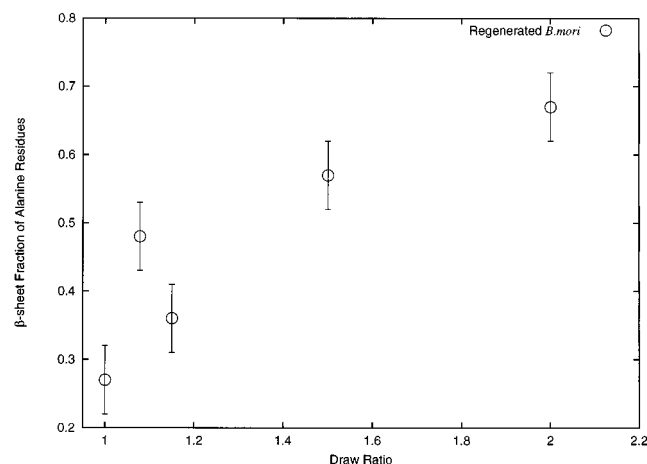


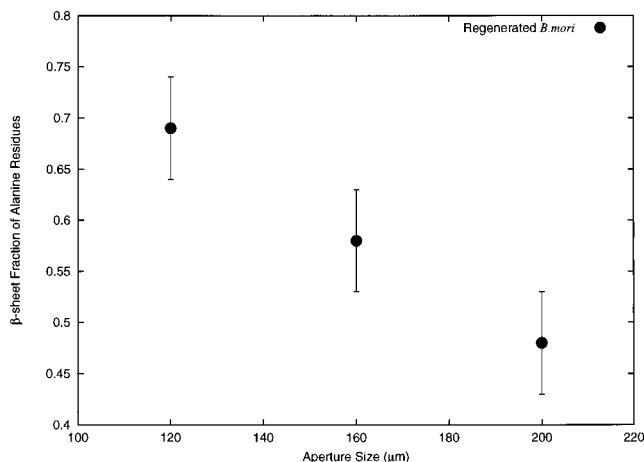
**Figure 6.** Relationship between the  $\beta$ -sheet fraction of the alanine residues and the draw ratio.

conformation; the one at 17.6 ppm is attributed to side chains in non- $\beta$ -sheet structures.<sup>3,4</sup>

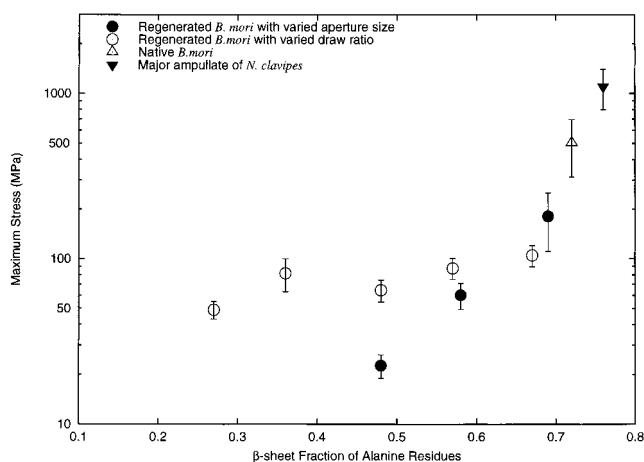
Figure 5 shows an expanded view of the methyl regions of alanine for native *B. mori* and for three representative samples of regenerated silk. The dotted lines in Figure 5 are the calculated spectra using the two Gaussians, whose parameters are used to calculate the  $\beta$ -sheet fraction. As can be seen in the figure, the native *B. mori* (a) has the most signal from the region near 20.4 ppm and the least from the 17.4 ppm region. The next three spectra, Figure 5 b,c,d, have progressively less  $\beta$ -sheet content.

Figure 6 displays the relationship between the  $\beta$ -sheet fraction of alanine residues and the draw ratio. All of these samples used the same spinneret aperture size of 140  $\mu\text{m}$ . The data suggest that the larger draw ratios produce a larger fraction of alanines in  $\beta$ -sheet conformations.

The other parameter that was studied was the aperture size. Figure 7 displays the relationship between the  $\beta$ -sheet fraction of the alanine residues and the aperture size of the spinneret. The relationship is linear over the range studied.



**Figure 7.** Relationship between the  $\beta$ -sheet fraction of the alanine residues and the size of the aperture used.



**Figure 8.** Relationship between the average maximum stress and the  $\beta$ -sheet fraction of the alanine residues. Each data point represents the average of about 10–15 Instron samples and 8–30 mg of silk fibers for the NMR study.

Taken together, these results suggest that the final conformation of the silk protein is affected by these macroscopic processing parameters. Specifically, these processing parameters allow for the improvement of the  $\beta$ -sheet fraction, which contributes to the degree of crystallinity of the protein.

Our results are consistent with a recent paper that used Raman spectroscopy, circular dichroism, and X-ray diffraction to investigate the conformation of synthetically spun fibers of *B. mori* spun using a somewhat different apparatus. They also found an increase in  $\beta$ -sheet content with increasing draw ratio.<sup>10</sup> Our work is complementary in that it identifies alanines as the molecular entity responsible for the  $\beta$ -sheets.

**Correlation between Maximum Stress and  $\beta$ -Sheet Fraction.** Figure 8 shows the relationship between the average stress and the  $\beta$ -sheet fraction of alanines from three different types of silk fibers (regenerated *B. mori*, native *B. mori*, and the major ampullate gland silk of the spider *N. clavipes*). This chart shows that a steep increase of the fiber's maximum stress is achieved at  $\beta$ -sheet fractions greater than 0.65. Figure 8 suggests that a high ( $>0.65$ )  $\beta$ -sheet fraction is a necessary component of high-stress silk fibers. However, these data do not suggest that the  $\beta$ -sheet fraction is the only parameter in determining the maximum stress of the fibers. There are a few data points (notably

at  $\beta$ -sheet fractions of 0.48 and 0.57) where samples have very similar  $\beta$ -sheet fractions yet their stress varied considerably. It is likely that the degree of orientation also contributes to the mechanical properties of the fibers.

### Conclusions

The design and fabrication have been described of a microfabricated spinneret that can routinely produce fibers from as little as 10 mg of protein. The spinneret has been demonstrated to be a useful tool for small-scale protein fiber research and development. This manuscript describes the routine production of about 10 mg of fiber per run. This is essential for production of fiber samples that can be varied in some processing parameter and yet still have large enough samples that are amenable to characterization by NMR and mechanical testing. Simple modifications to eliminate dead volume could easily reduce by a factor of 2 the amount of protein required. This technology is attractive in that it allows for the development and design of genetically engineered protein fibers without the necessity of producing large quantities of protein for each trial.

As the diameters of the regenerated fibers approach that of the native silk fibers (Figure 3), the mechanical properties of the regenerated silk fibers converge on the native silk fiber properties. The higher maximum stress and lower maximum strain as the diameter decreases is attributed to an overall increase in orientation. The macroscopic processing parameters have control over the conformation of the protein. Both decreasing aperture size and increasing draw ratios increase the  $\beta$ -sheet fraction of the alanine residues in the silk fibers.

A high ( $>0.65$ )  $\beta$ -sheet fraction is a necessary component of high-stress fibers. However,  $\beta$ -sheet fraction is not the unique determinant of maximum stress of the silk fibers; it is suggested that crystallite orientation is also important.

**Acknowledgment.** The authors acknowledge the support of NSF grants DMR-9708062 and MCB-9601018. O.L. acknowledges the support of the NIH Training Grant in Molecular Physics of Biological Systems (NIH T32GM08267). In addition, the authors thank Professor Peter Scwhartz and Professor Robert Austin for insightful discussions.

### References and Notes

- (1) Prince, J. T.; McGrath, K. P.; DiGirolamo, C. M. and Kaplan, D. *Biochemistry* **1995**, *34*, 10879–10885.
- (2) Lewis, R. V.; et al. *Protein Expression Purification* **1996**, *7*, 400–406.
- (3) Wishart, D.; Sykes, B. D. *J. Biomol. NMR* **1994**, *4*, 171–180.
- (4) Saito, H. *Magn. Reson. Chem.* **1986**, *24*, 835–852.
- (5) Lock, R. L. Process for making silk fibroin fibers, US Patent 5,252,285, October 1993.
- (6) Gay, J.; Gay, D.; Welsh, R. *ACM Trans. Math. Software* **1981**, *7*, 369–383.
- (7) Jenkins, A. *Polymer Science*; North-Holland; Amsterdam, 1972.
- (8) Sawyer, L. C.; Jaffe, M. *J. Mater. Sci.* **1986**, *21*, 1897–1913.
- (9) Baer, E.; Moet, A. *High Performance Polymers*; Hanser Publishers: Munich, 1991.
- (10) Trabbic, K. A.; Yager, P. *Macromolecules* **1998**, *31*, 462–471. This paper appeared while our paper was under review.

MA971626L